Anomalous expansion of Nb nanowires in a NiTi matrix under high pressure

Cun Yu, Yang Ren, Lishan Cui' , Zhiyuan Ma, and Wenge Yang'

Citation: Appl. Phys. Lett. **109**, 161903 (2016); doi: 10.1063/1.4965117
View online: http://dx.doi.org/10.1063/1.4965117
View Table of Contents: http://aip.scitation.org/toc/apl/109/16
Published by the American Institute of Physics

Anomalous expansion of Nb nanowires in a NiTi matrix under high pressure

Cun Yu,[1,2] Yang Ren,[3] Lishan Cui,[1,a)] Zhiyuan Ma,[1] and Wenge Yang[4,5,a)]
[1]*Department of Materials Science and Engineering, China University of Petroleum-Beijing, Beijing 102249, China*
[2]*Shanghai Institute of Applied Physics, Chinese Academy of Sciences (CAS), Shanghai 201800, China*
[3]*X-ray Science Division, Argon National Laboratory, Argonne, Illinois 60439, USA*
[4]*Center for High Pressure Science and Technology Advanced Research (HPSTAR), Shanghai 201203, People's Republic of China*
[5]*High Pressure Synergetic Consortium (HPSynC), Geophysical Laboratory, Carnegie Institution of Washington, Argonne, Illinois 60439, USA*

(Received 23 June 2016; accepted 5 October 2016; published online 17 October 2016)

Under high pressure, materials usually shrink during compression as described by an equation of state. Here, we present the anomalous volume expansion behavior of a one-dimensional Nb nanowire embedded in a NiTi transforming matrix, while the matrix undergoes a pressure-induced martensitic transformation. The Nb volume expansion depends on the NiTi transition pressure range from the matrix, which is controlled by the shear strain induced by different pressure transmitting media. The transformation-induced interfacial stresses between Nb and NiTi may play a major role in this anomaly. Our discovery sheds new light on the nano-interfacial effect on mechanical anomalies in heterogeneous systems during a pressure-induced phase transition. *Published by AIP Publishing.*
[http://dx.doi.org/10.1063/1.4965117]

Strength and compressibility are fundamental material properties. Under compression, the volume of studied materials usually decreases with increasing applied pressure, following an "equation of state" (EoS), which describes volume change in response to an applied pressure. A martensitic transformation is the first order transformation of a diffusionless lattice distortion, where a solid's volume change decreases abruptly under high pressure with a rapid mechanical shock wave (i.e., speed of sound), irrespective of the applied pressure (i.e., high pressure-induced martensitic transformation of iron).[1,2] Recent reports show that Nb nanowires embedded in a NiTi matrix with martensiric transformation exhibited an ultra-large elastic deformation and the unique characteristic of rapidity, dictated by the martensitic transformation of the NiTi matrix under uniaxial tension.[3] In this nanocomposite, a large shear strain (6%–8%) was induced along the loading direction once the martensitic transformation of the NiTi matrix was triggered by shear stress.[4] In addition, Nb presents high-pressure structural stability with no structural phase transition under pressures up to 145 GPa.[5] Therefore, we speculate that the compression behavior of this nano-component embedded in a transforming matrix is also influenced by the martensitic transformation of the matrix under high pressure and may give abnormal results. In order to verify this, we carried out a high-pressure study on a nanocomposite containing Nb nanowires and a NiTi-shape memory alloy (SMA) matrix. Studying the pressure effect on these multiple phase heterogeneous systems is also very interesting. By varying the pressure transmitting media, we were able to control the shear stress magnitude to trigger the martensitic transition pressure, maintain both co-existing parent austenite and martensitic phases in a wide range, and study the interfacial effect on the mechanical response of the Nb nanowires embedded in the matrix under high pressure.

An ingot with a composition of $Ni_{47}Ti_{44}Nb_9$ (at. %) was prepared by vacuum induction melting.[3] The wires of the composite with a diameter of 0.5 mm were subsequently fabricated by forging, wire-drawing, and annealing. In order to obtain a fine composite powder for x-ray diffraction (XRD) characterization, we hydrogenated the macroscopic wire at room temperature (25 °C) and then ground it into micro-sized particles (1–5 μm). Finally, the composite particles were de-hydrogenated at 500 °C in a vacuum. The typical microstructure of this composite is shown in Fig. 1. Nb nanowires with a mean diameter of 20–40 nm are well dispersed in the NiTi matrix and aligned along the wire-drawing direction (Fig. 1(a)), with semi-coherent interfaces (Fig. 1(b)).

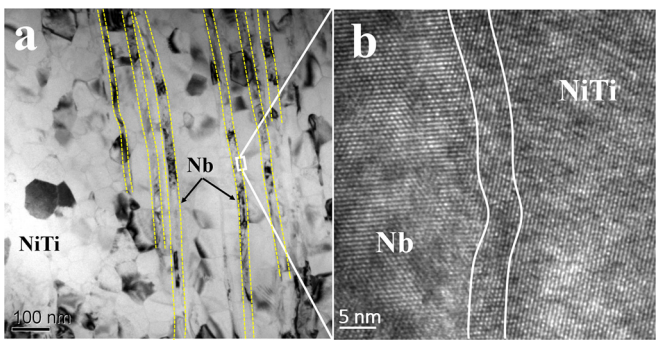

FIG. 1. Microstructure characterization of the Nb/NiTi nanocomposite system. (a) Transmission electron microscopy (TEM) image of the longitudinal section of the composite wire. The dashed lines indicate the boundaries of the Nb nano-rods and NiTi substrate. The typical width of the 20 nm Nb nano-rods is clearly dispersive in the substrate. (b) High-resolution TEM image of the interface between the NiTi substrate and Nb nano-fiber. The white lines are a visual aid for the defect-free transition zone between the NiTi lattice and Nb lattice.

[a)]Authors to whom correspondence should be addressed. Electronic addresses: lscui@cup.edu.cn and yangwg@hpstar.ac.cn

We performed *in-situ* high-pressure synchrotron x-ray diffraction (XRD) experiments at beamline 16-BM-D, at the Advanced Photon Source. The typical two-dimensional (2D) XRD pattern in Fig. 2(a), at the initial pressure of 0.8 GPa after gas loading, with neon as our pressure transmitting medium, clearly shows the coexisting cubic Nb, austenite (B2) and martensite (B19′) phases of NiTi. Our high-pressure experiment reached 32 GPa. Fig. 2(b) shows three selected diffraction profiles at 0.8 GPa, 12.5 GPa, and 32 GPa. The complete profiles are shown in Fig. S1 (supplementary material). The NiTi-B2 cubic phase started to transfer to the B19′ phase at ~12.7 GPa, evidenced by the reducing and increasing intensity of $(110)_{B2}$ and $(111)_{B19'}$, respectively. A martensitic transformation in a NiTi-shape memory alloy (SMA) is triggered by a very low uniaxial stress (hundreds of mega-Pascal[4]). The initial small portion of the B19′ phase at 0.8 GPa is probably formed during the grinding preparation. The neon pressure medium provides fairly good hydrostatic pressure conditions until ~12.7 GPa before the neon pressure medium begins to develop non-hydrostatic conditions in the sample chamber,[6] where shear stress triggers the B2→B19′ transition. As pressure increases, the B19′ phase portion increases by consuming the B2 phase. Even at the highest pressure of 32 GPa studied here, there are still a few remaining intensities from the $(211)_{B2}$ and $(110)_{B2}$ reflections (Fig. 2(b)), which indicates a very small shear stress build up inside the sample chamber at 32 GPa. In this case, the long sluggish NiTi martensitic transition is very similar to the transformation behavior of iron under a good hydrostatic pressure medium.[1] The XRDs from the Nb nano-fibers show no structural transition in the entire pressure range.

A summary of the compression behavior of the Nb nanowires at high pressure is displayed in Fig. 3. Fig. 3(a) presents the $(110)_{Nb}$, $(200)_{Nb}$, and $(211)_{Nb}$ d-spacings versus pressure. The main reflection of $(110)_{Nb}$ overlapped with three other peaks from the NiTi-B2 and B19′ phases, and multi-peak fitting was applied to these four peaks, as demonstrated in Fig. S2 (supplementary material). The other two peaks of the Nb phase, $(200)_{Nb}$, and $(211)_{Nb}$, were fitted using the Gaussian function separately. The relative change of the d-spacings shown in Fig. 3(a) is consistent with that found in unconstrained bulk Nb from the beginning (at 0.8 GPa) to 14.7 GPa[5]], suggesting that the compression behavior of the Nb phase is unaffected by the NiTi matrix during this stage. Surprisingly, the d-spacings of all these three lattice planes started to increase after 17.6 GPa and then decreased again when the applied pressure exceeds 21.4 GPa. Even at the highest pressure of 32 GPa, this is still much higher than the normal compression curve extended by the low-pressure compression curve (the regular equation of state with the dashed line) while the martensitic transition is incomplete. The volume expansion of a single-phase system under high pressure has never been reported before for the favorite of energy term from P·V (pressure·volume). For comparison, we also conducted the same experiment using silicon oil as our pressure medium, which generates a non-hydrostatic condition at much lower pressure. The anomalous volume expansion of the Nb nanowires was much more pronounced when pressure surpassed 10 GPa (Fig. S3 of supplementary material) and significant shear stress built up in the pressure-transmitting medium (silicone oil). As reported in Ref. 6, Neon crystallizes at 4.8 GPa at room temperature, and the first signs of non-hydrostaticity appear at around 15 GPa; but for silicone oil, nonhydrostaticity starts to strengthen around 10 GPa. In both cases, the shear stress builds up high enough to trigger the NiTi martensitic phase transition at 15 GPa and 10 GPa for Neon and silicone oil, respectively. It is clear that the anomalous compression behavior of Nb is directly driven by the interfacial stress from the martensitic transformation of the NiTi matrix (Fig. S3 of supplementary material).

Fig. 3(b) shows the pressure-volume (P-V) relation of the Nb phase and corresponding fitting and calculation results. We calculated the unit cell volume of the cubic structure Nb phase based on the (110), (200), and (211) lattice spacings. The data from 0.8 GPa (the first data point) to 10 GPa are fitted by the third-order Birch-Murnaghan equation of state (EOS)[7]

$$p = 1.5K\left[\left(\frac{v}{v_0}\right)^{\frac{-7}{3}} - \left(\frac{v}{v_0}\right)^{\frac{-5}{3}}\right] \times \left\{1 - 0.75(4 - K')\left[\left(\frac{v}{v_0}\right)^{\frac{-2}{3}} - 1\right]\right\}, \quad (1)$$

where $\frac{v}{v_0}$ is the ratio of the unit cell volume at pressure p to ambient pressure, K is the bulk modulus at ambient conditions, and K′ is its pressure derivative. The least-square fitting yields $K = (170 \pm 3)$ GPa, and $K' = (3.7 \pm 0.2)$, which also agrees with previous experimental reports and theoretical calculations.[8,9] The data outside the fitting region is an extrapolation from this EOS and plotted in a dashed line in

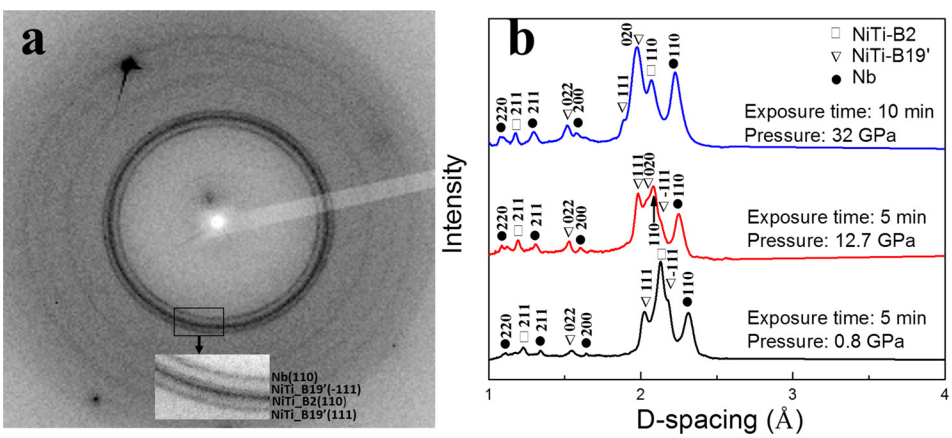

FIG. 2. *In-situ* X-ray diffraction (XRD) results of the composite powder under different pressures. (a) A 2D diffraction pattern at the initial pressure of 0.8 GPa. The inset shows an enlarged portion to clearly reveal the diffraction power rings from the bcc-Nb, B2-NiTi, and B19′-NiTi phases. (b) Integrated 1D diffraction patterns at 0.8 GPa, 12.7 GPa, and 32 GPa. Intensity from the B19′ phase starts to increase at 12.7 GPa, and a reasonable amount of the NiTi B2 phase exists up to 32 GPa, which indicates a little shear stress is generated by the solid Neon pressure medium, even at the highest pressure studied here (32 GPa).

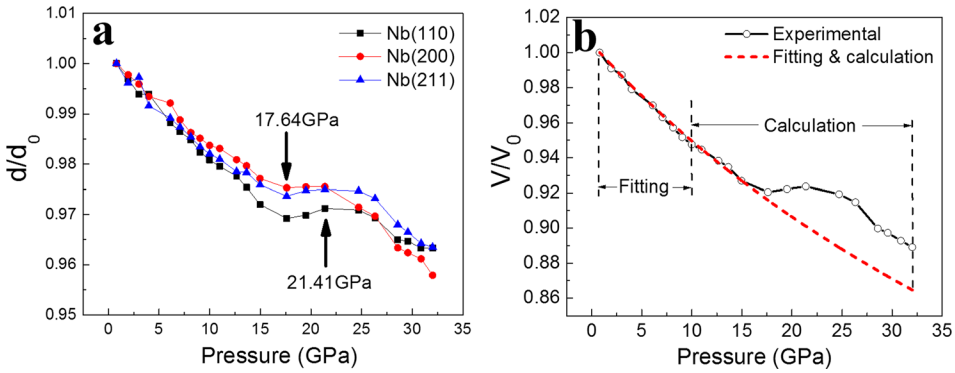

FIG. 3. Compression behavior of Nb nanowires with Neon as a pressure transmitting medium. (a) The pressure-d-spacing plots of three different crystallography planes. (b) The pressure-volume data of Nb (black line with hollow circles). The red dotted line represents the fitted result using the third order Birch-Murnaghan equation of state.

Fig. 2(d) as a reference. The unit cell volume of the Nb nanowires deviates obviously between the experimental data and calculation result beyond 17.64 GPa; especially, where a mild volume expansion occurs when pressure increases from 17.64 GPa to 21.41 GPa. In order to reveal the underlying mechanism of this abnormal volume expansion at high pressure, we analyze the pressure-induced martensitic transformation of the NiTi matrix and compression behaviors of the B2 and B19′ phases below.

Fig. 4 shows the progression of the pressure-induced phase transition from B2 to B19′ and the compression behaviors of the B2 and B19′ phases. The intensity evolution of $(110)_{B2}$ was used to characterize the extent of the phase transition, as shown in Fig. 4(a). It is clear that the NiTi matrix phase transition started at 12.7 GPa and lasted to ~30 GPa; however, the volume expansion of the Nb phase emerged at 17.64 GPa, when most of B2 phase had already transferred to the B19′ phase. If the NiTi phase transition triggered the volume expansion of Nb, they should happen at the same pressure. One possibility is that the martensitic transformation of the NiTi matrix is discontinuous due to the inhibition of the Nb nanowires and only partial B2 grains transfer to the B19′ phase initially due to mild shear strain induced by the Neon pressure medium. Thus, only a small portion of the Nb nanowires next to the B19′ grains expand while the rest remain under compression. On average, the d spacings of the lattice planes of both Nb and NiTi (including B2 and B19′) still shrink, but slightly deviate from the ideal compression curve. Fig. 4(b) shows the relative compression rates of the NiTi-B2 and NiTi-B19′ phases, represented by the d-spacing evolutions of $(110)_{B2}$ and $(111)_{B19'}$, respectively. From the beginning to 17.64 GPa, the relative d spacing of $(111)_{B19'}$ remains almost consistent with $(110)_{B2}$, suggesting they share a uniform deformation behavior. Beyond 17.64 GPa, most of the B2 phase transforms to the B19′ phase, an anomalous lattice plane expansion is also observed in $(110)_{B2}$, and meanwhile the B19′ phase shows a much steeper compression ratio due to the softening transformation.

Fig. 5 shows a series of schematic diagrams to illustrate the underlying micro-mechanism of the anomalous volume expansion behavior of Nb. The studied composite sample contained thousands of Nb nano-wires. We defined two macroscopic directions that correspond to the longitudinal (LD) and transverse directions (TD) of the Nb nanowires' drawing direction at the sample preparation stage. In the low-pressure region (Fig. 5(a)), three phases coexist in the composite particle: NiTi-B2 (major phase, blue area), NiTi-B19′ (minor phase, blue shadow), and Nb nano-rod (orange area). With increasing pressure (Fig. 5(b)), the NiTi-B2 phase begins to transform to the NiTi-B19′ phase from ~12.7 GPa and the corresponding lattice changes from a cubic (Pm-3m) to a monoclinic ($P2_1/m$) structure. During this martensitic transformation, shear deformation produces an elongation strain. Following the texture analysis on the studied materials, the NiTi-B2 phase shows a ⟨111⟩ fiber texture and the Nb nanowires present a strong ⟨110⟩ fiber texture in the LD (Fig. S4 of supplementary material). It is reasonable to believe the crystallographic relationship between NiTi-B2 and Nb is mainly $(111)_{B2} \parallel (110)_{Nb}$. It is well known that the relationship between B2 and transformed B19′ is $(111)_{B2} \leftrightarrow (021)_{B19'}$ based on the crystallographic relationship of the martensitic transformation.[10] At ambient pressure, the d-spacing of $(021)_{B19'}$ (0.1878 nm from PDF card 65-7711) is 8% longer than $(111)_{B2}$ 0.1740 nm from PDF card 18-0899). In addition, we calculated the d-spacing of $(021)_{B19'}$ and $(111)_{B2}$, which is 0.1750 nm and 0.1484 nm, separately under the high pressure of ~12.7 GPa (the elastic moduli of $(021)_{B19'}$ and $(111)_{B2}$ are 187 GPa and 86.3 GPa, respectively[11]). Apparently, an

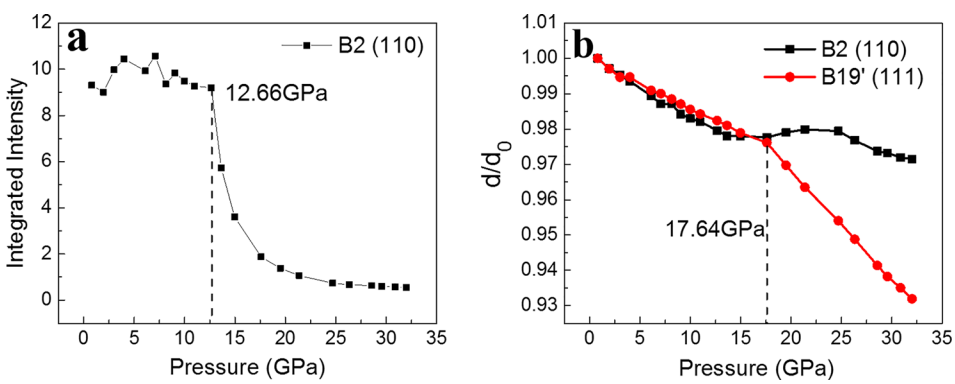

FIG. 4. Compression behavior of the NiTi matrix. (a) Intensity of NiTi-B2 (110) reflection versus pressure. From 14.7 GPa to 17.4 GPa, a fast reduction in the diffraction intensity of the B2(110) reflection is observed. (b) The relative d-spacing of B2 (110) and B19′ (111) reflections versus pressure. Beyond 17.4 GPa, the B19′ (111) lattice decreases more rapidly than the low-pressure compression rate, while the B2 (110) lattice shows a similar anomalous compression behavior to the Nb nano-rods.

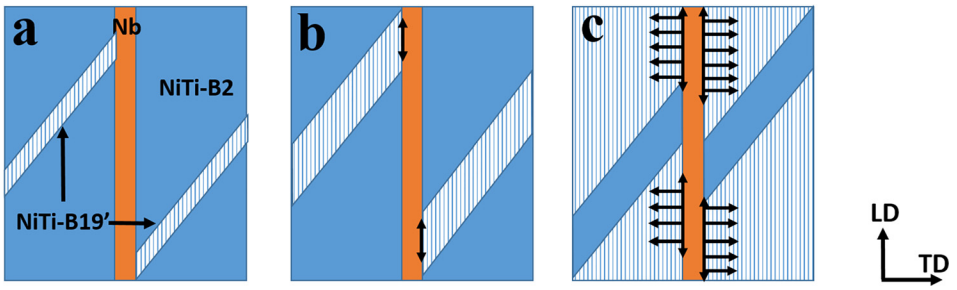

FIG. 5. Schematic diagrams show the internal stress evolution during the NiTi matrix phase transformation. (a) Three phases (B2, B19′ and Nb) coexist at the initial state of the composite under the just-loaded pressure of 0.8 GPa. (b) The beginning of the phase transformation from NiTi-B2 to B19′ at 12.7 GPa. (c) Most of the B2 phase has transformed to the B19′ phase at 17.64 GPa.

elongation is produced by phase transformation (B2→B19′) in the LD and consequently, the adjacent Nb nanowires are under tensile strain in the LD due to the interface shear stresses, as shown in Fig. 5(b) (double arrows). In the TD, internal stresses (indicated by a series of single arrows shown in Fig. 5(c)) are produced by an abrupt change in the NiTi matrix compressibility due to phase transformation softening. It is known that the tangent modulus of NiTi during transformation is close to zero.[12] Moreover, the bulk modulus and Young's modulus of the B19′ phase are both smaller than the B2 phase.[13] During the initial stage of transformation (from 12.6 GPa to 17.64 GPa), the compressibility of the NiTi matrix is dominated by the B2 phase, because the discontinuously-transformed B19′ phase is constrained by the B2 phase, as evidenced by the uniform-deformation behavior of both phases, shown in Fig. 5(b). Thus, transformation softening is hindered at this stage. Once pressure exceeds 17.64 GPa, most of the B2 phase has transformed to the B19′ phase (Fig. 5(c)) and the constraint is released as evidenced by the abrupt change in the compression ratio of $(111)_{B19'}$, shown in Fig. 4(b). Subsequently, the interface stress in the TD is produced by the intense contraction of the B19′ phase due to transformation softening and bulk modulus reduction (from B2 to B19′). The internal stress also leads to an elongation of the Nb nanowires in the TD. In conclusion, internal interface stress during the last stage of transformation (from 17.64 GPa to 21.41 GPa) expands the unit cell volume of the Nb phase. As pressure increases continuously, the transformation effects weaken as the phase transition ends and the volume of the Nb phase decreases again.

In summary, we observed the anomalous compression behavior of Nb nanowires embedded in a NiTi matrix during the NiTi martensite transition. The volume of the Nb nanowires showed a mild expansion from 17.64 GPa to 21.41 GPa with a good hydrostatic pressure medium (Neon), and an abrupt expansion at much lower pressure with a high viscosity pressure medium (silicone oil). This volume expansion was triggered by the martensitic transformation of the NiTi matrix that emerged at 12.7 GPa. The volume expansion of Nb observed in the Nb/NiTi composite at higher pressure uncovers the nanoscale interfacial effect on the mechanical properties of the nano-structured composite under high pressure. This study provides direct evidence of the underlying micro-mechanism of multiphase alloys' compression behaviors and promotes the design of materials in a high-pressure environment.

A Mao-Bell type symmetric diamond-anvil cell, with a pair of 300 μm culet sized diamond anvils, was used to generate a high-pressure environment for a Nb nanowire embedded in a NiTi alloy. A 100 μm diameter hole was drilled at the center of the stainless steel gasket and preindented to a thickness of around 40 μm to form the sample chamber. The compressed composite powder pellet (about 40 μm L × 20 μm W × 20 μm H) was loaded in the center of the sample chamber with a Neon pressure transmitting medium. We used three ruby spheres (5–8 μm in diameter) as our pressure standards, placed in different positions to monitor the pressure distribution inside the sample chamber (Fig. S5 of supplementary material). For comparison, we also prepared one cell with a similar geometry but used silicone oil as the pressure medium instead.

In-situ high-pressure XRD measurements were carried out at the 16BM-D station of the High-Pressure Collaborative Access Team (HPCAT), at the Advanced Photon Source, Argonne National Laboratory. The monochromatic x-ray beam at wavelength 0.3444 Å was focused to ~15 μm (vertical) × 5 μm (horizontal) in full width at half maximum (FWHM). The diffraction patterns were collected using a MAR345 image plate, with a typical exposure time of 5–10 min. Each diffraction pattern was collected after the pressure was adjusted and stabilized to ensure steady pressure during our XRD measurements. The two-dimensional diffraction patterns were integrated with the FIT2D program to produce diffraction profiles of intensity versus d-spacing.

See supplementary material for an A series of XRD patterns at different pressures; a detailed analysis of the XRD patterns, and compression behavior of Nb nanowires with silicon oil as a pressure-transmitting medium; inverse pole figures of the NiTi matrix and Nb nanowires; and an optical microscopy image of the samples.

The authors acknowledge the support of the National Natural Science Foundation of China (NSFC) (Grant Nos. 51231008, 11474362, and U1530402). HPCAT operations are supported by DOE-NNSA under Award DE-NA0001974 and DOE-BES under Award DE-FG02-99ER45775, with partial instrumentation funding by NSF. The gas loading was performed at GeoSoilEnviroCARS, APS, ANL, supported by EAR-1128799 and DE-FG02-94ER14466. Use of the Advanced Photon Source was supported by the U. S. Department of Energy, Office of Science, Office of Basic Energy Sciences, under Contract No. DE-AC02-06CH11357.

[1]P. M. Giles, M. H. Longenbach, and A. R. Marder, J. Appl. Phys. **42**, 4290 (1971).
[2]W. A. Bassett and E. Huang, Science **238**, 780 (1987).
[3]S. Wang, L. Cui, S. Hao, D. Jiang, Y. Liu, Z. Liu, S. Mao, X. Han, and Y. Ren, Sci. Rep. **4**, 6753 (2014).

[4]K. Otsuka and X. Ren, Prog. Mater. Sci. **50**, 511–678 (2005).
[5]T. Kenichi and A. K. Singh, Phys. Rev. B **73**, 224119 (2006).
[6]S. Klotz, J. C. Chervin, P. Munsch, and G. Le Marchand, J. Phys. D: Appl. Phys. **42**, 075413 (2009).
[7]F. Birch, J. Geophys. Res. Solid Earth **83**(B3), 1257–1268, doi:10.1029/JB083iB03p01257 (1978).
[8]Y. Song, R. Yang, D. Li, W. T. Wu, and Z. X. Guo, Phys. Rev. B **59**, 14220 (1999).
[9]M. J. Mehl and D. A. Papaconstantopoulos, Phys. Rev. B **54**, 4519 (1996).
[10]O. Matsumoto, S. Miyazaki, K. Otsuka, and H. Tamura, Acta Metall. **35**, 2137 (1987).
[11]P. Sittner, L. Heller, J. Pilch, C. Curfs, T. Alonso, and D. Favier, J. Mater. Eng. Perform. **23**, 2303–2314 (2014).
[12]Y. Liu and H. Xiang, J. Alloys Compd. **270**, 154–159 (1998).
[13]M. F. X. Wagner and W. Windl, Acta Mater. **56**, 6232–6245 (2008).